

UNSTEADY CHARACTERISTICS OF TIP-LEAKAGE FLOW IN AN AXIAL FLOW FAN

Keuntae Park

Department of Mechanical & Aerospace Engineering
Seoul National University
1 Gwanak-ro, Gwanak-gu, Seoul, 08826, Korea
ojirab@snu.ac.kr

Haecheon Choi

Department of Mechanical & Aerospace Engineering
Seoul National University
1 Gwanak-ro, Gwanak-gu, Seoul, 08826, Korea
choi@snu.ac.kr

Seokho Choi

Air Conditioning R&D Lab.
LG Electronics
51 Gasan digital 1-ro, Geumcheon-gu, Seoul, 08592, Korea
seokho.choi@lge.com

Yongcheol Sa

Air Conditioning R&D Lab.
LG Electronics
51 Gasan digital 1-ro, Geumcheon-gu, Seoul, 08592, Korea
yongcheol.sa@lge.com

Oh-kyoung Kwon

National Institute of Supercomputing and Networking
Korea Institute of Science and Technology Information
245 Daehak-ro, Yuseong-gu, Daejeon, 34141, Korea
okkwon@kisti.re.kr

ABSTRACT

An axial flow fan with a shroud generates complicated tip-leakage flow by the interaction of the axial flow with the fan blades and shroud near the blade tips. In this study, large eddy simulation (LES) is performed for tip-leakage flow in a forward-swept axial flow fan inside an outdoor unit of an air-conditioner, operating at the design condition of the Reynolds number of 547,000 based on the radius of blade tip and the tip velocity. A dynamic global model (Lee et al., 2010) is used for a subgrid-scale model, and an immersed boundary method in a non-inertial reference frame (Kim and Choi, 2006) is adopted. The present simulation reveals the evolution of tip-leakage vortex (TLV) near the blade tip. After inception of TLV near the leading edge of the suction-side of the blade tip, it develops downstream, and migrates toward the pressure surface of the following blade. Along the trajectory of the TLV, the turbulent kinetic energy and pressure fluctuations are high due to the oscillatory feature of the TLV. Energy spectra of the velocity fluctuations near the following blade and the trajectory of the TLV indicate that the TLV shows low-frequency wandering movement.

INTRODUCTION

The axial flow fan is one of the most widely used axial turbomachines for cooling and ventilation in various engineering applications. In the axial flow fan, the tip-leakage flow is inevitable due to the tip-clearance for its operation. It is driven by the pressure difference between the pressure and suction sides of the blade tip and is responsible for a substantial aerodynamic loss in the axial flow fan. Also rotating instabilities, blockages, and broadband noise emissions are induced by the tip-leakage flow.

In recent years, researches are performed either experimentally or numerically to achieve a better understanding of unsteady phenomena of the tip-leakage flow in axial turbomachines. Miorini et al. (2012) experimentally investigated the internal structures of the tip-leakage vortex (TLV) within the rotor of an axial water-jet pump using particle image velocimetry (PIV). They observed that the instantaneous TLV is composed of unsteady vortex filaments which shed at the tip from the leakage flow. More recently, they measured the flow in the tip region of a subsonic compressor rotor for two flow rates to characterize the location, trajectory, and behavior of the tip leakage vortex (Tan et al., 2015). Jin et al. (2013) conducted PIV and wall pressure test

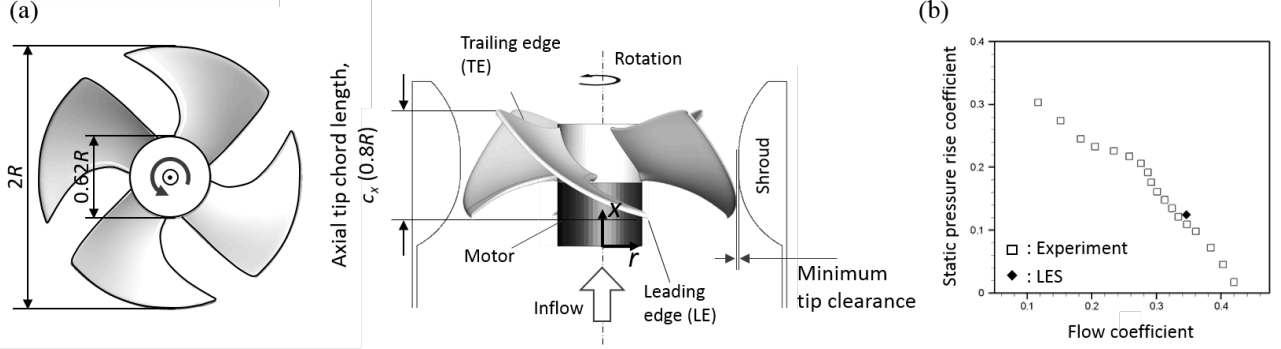


Figure 1. (a) Front and lateral views of the axial flow fan; (b) Performance curve of the axial flow fan. In (b), closed symbol indicates the result from the present simulation.

in axial fans to investigate the effect of sweep on unsteady characteristics of tip-leakage flow.

With the rapid development of computing power, large eddy simulations (LES), a good compromise method between the direct numerical simulation (DNS) and the RANS simulation, have been applied to investigate unsteady characteristics of tip-leakage flow in a linear cascade of an axial compressor (You et al., 2007), in a one and half stage compressor (Hah et al., 2015), and in a blade passage of an axial fan (Jang et al., 2001; Boudet et al., 2015; Pogorelov et al., 2015). Although much progress has been made by previous studies, the detailed dynamics of the tip-leakage flow is still not fully understood. Especially the flow in an axial flow fan is less concerned than those in other axial turbomachines such as pump, compressor and turbine.

In the present work, we conduct LES of the flow in a forward-swept axial flow fan to investigate the unsteady characteristics of the tip-leakage flow. The Reynolds number at the design condition is $Re = 547,000$ based on the radius of the blade tip (R) and the tip velocity (U).

TEST AXIAL FLOW FAN

The present simulation is performed for a forward-swept axial flow fan with an inlet duct and a converging-diverging nozzle type shroud covering the entire region of the fan blade (Fig. 1(a)). It has a minimum tip clearance of 3.6% of the wing tip radius. This configuration is based on a simplified model of an outdoor unit of an air-conditioner. An operating design condition with a flow coefficient of $\Phi = Q/\pi R^2 U = 0.346$ and $Re = 547,000$ is investigated. The performance curve is shown in Fig. 1(b). The static pressure rise coefficient from the present LES at the design condition is also marked in Fig. 1(b).

NUMERICAL METHODOLOGY

Simulations are performed in a non-inertial reference frame that rotates with the axial flow fan. The governing equations in the non-inertial reference frame for LES are spatially filtered Navier-Stokes and continuity equations:

$$\frac{\partial \bar{u}_i}{\partial t} + \frac{\partial}{\partial x_j} (\bar{u}_j \bar{u}_i - \nu_j \bar{u}_i + \bar{u}_j w_i) = -\frac{\partial \bar{p}}{\partial x_i} + \frac{1}{Re} \frac{\partial^2 \bar{u}_i}{\partial x_j \partial x_j} - \frac{\partial \tau_{ij}}{\partial x_j} + f_i \quad (1)$$

$$\frac{\partial \bar{u}_i}{\partial x_i} - q = 0 \quad (2)$$

where $u_i = u_{r,i} + \varepsilon_{ijk} \Omega_j x_k + u_{s,i}$, $v_i = \varepsilon_{ijk} \Omega_j x_k + u_{s,i}$, and $w_i = \varepsilon_{ijk} \Omega_j x_k$. All the terms are written in a strongly conservative form and all the variables are non-dimensionalized by the radius of the blade tip and the tip velocity. The subgrid-scale stress tensors (τ_{ij}) are modelled using a dynamic global model (Park et al., 2006; Lee et al., 2010). This model provides zero subgrid-scale dissipation for some laminar shear flows and a dynamic procedure for the model coefficient which is globally constant in space but varies only in time without any *ad hoc* clipping. For implementing no slip boundary conditions at the moving body surface, we use the immersed boundary (IB) method in a non-inertial reference frame (Kim and Choi, 2006). In (1) and (2), f_i and q , respectively, are the momentum forcing and the mass source/sink defined on the immersed boundary or inside the body. The detailed procedures to determine these are given in Kim and Choi (2006). Compared to the body-fitted methods, this method greatly simplifies the grid generation for complex geometries. Posa et al. (2011) also reported an application of the IB method for simulation of flow in a rotating machinery.

The above equations are solved in the cylindrical coordinate system using a second-order semi-implicit fractional-step method proposed by Akselvoll and Moin (1996). For the spatial discretization, a hybrid scheme with a third-order QUICK scheme upstream of the leading edge of the motor ($x/R < 0$) and the second-order central difference scheme elsewhere is applied.

At the duct inlet ($x/R = -4.29$, $r/R \leq 1.36$), we prescribe a top-hat velocity profile without background disturbances. At the lateral and outflow boundaries, the Neumann boundary conditions are imposed. A sponge layer with the grid stretching in the axial direction and the explicit 1:2:1 filtering for all velocity components in all directions are adopted to attenuate disturbances near the outflow boundary (Fig. 2). Boundary conditions on blades and a hub are specified with $\mathbf{u} = \boldsymbol{\Omega} \times \mathbf{x}$, while those on the shroud, duct, and wall are prescribed with $\mathbf{u} = \mathbf{0}$.

The computational grid consists of $769 \times 679 \times 1536$ points in the axial (x), radial (r) and azimuthal (θ) directions, respectively (a total of 802 million). In the tip clearance, the ratio of the minimum grid spacing on the shroud wall to the blade radius is

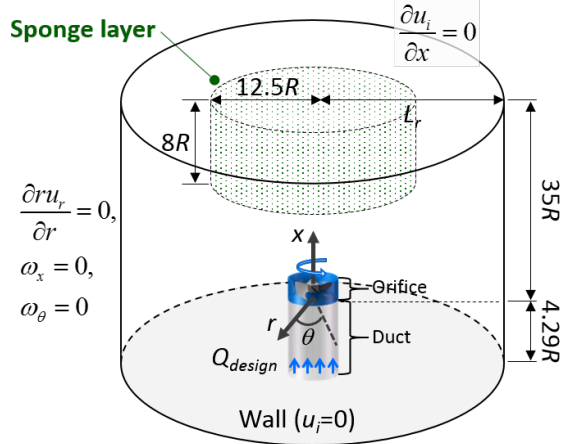


Figure 2. Schematic diagram of the coordinates, computational domain, and boundary conditions

5×10^{-4} . This minimum grid spacing corresponds to $\Delta y^+ \sim 10$ near the tip clearance. To handle the massive grids, MPI parallel computation with a 2D domain decomposition is applied using 2048 cores of the Tachyon II (Intel Xeon X5570 2.93 GHz) at the KISTI supercomputing center, Korea.

RESULTS AND DISCUSSION

The static pressure rise coefficient predicted by the present LES is compared with the experimental result from a fan test rig (Fig. 1(b)). The predicted value has excellent agreement with the experimental one. In the following, we discuss vortical structures near the blade tip and unsteady characteristics of the TLV.

A. Vortical Structures near the Blade Tip

In Fig. 3, passage-averaged vortical structures are illustrated using the iso-surface of the λ_2 (Jeong and Hussain, 1995) colored with the helicity normalized by the angular velocity Ω and relative velocity magnitude $|\mathbf{u}_r|$, $\omega_s = \boldsymbol{\omega} \cdot |\mathbf{u}_r| / 2\Omega |\mathbf{u}_r|$, where $\boldsymbol{\omega}$ is the absolute vorticity. As shown, vortical structures such as tip-leakage vortex (TLV), blade wake and edge separation are found. Among them, the TLV with negative ω_s is the predominant flow structure in the passage. It is initiated near the leading edge of the suction side of the blade tip and migrates to the pressure side of the following blade. The negative value of streamwise vorticity indicates that the TLV rotates in the clockwise direction when viewed from downstream.

Distributions of the turbulent kinetic energy and rms pressure fluctuations are shown in Fig. 4, together with the trajectory of the TLV in the passage. The core of the λ_2 iso-surface is used to identify the trajectory of the TLV. The region with high turbulent kinetic energy coincides with the core of the TLV, whereas the pressure fluctuations are high in the left and right regions (in the azimuthal direction) of the TLV core. This implies that the TLV contains high turbulent kinetic energy and oscillates in the azimuthal direction.

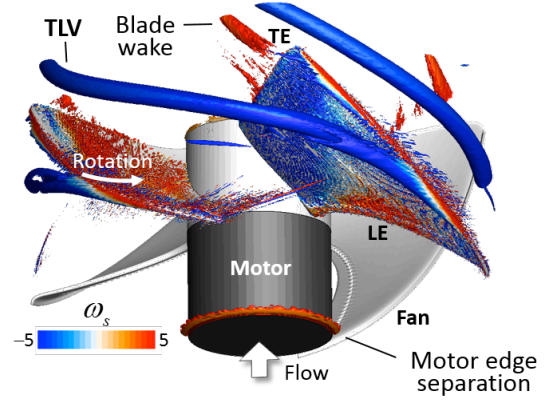


Figure 3. λ_2 iso-surface colored with a normalized helicity from passage-averaged flow field.

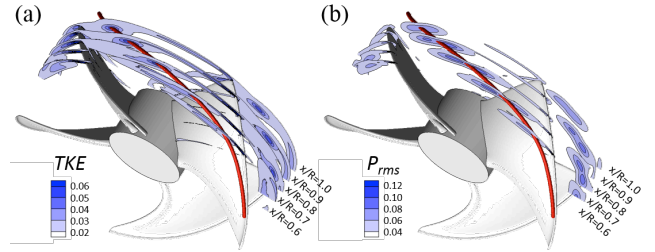


Figure 4. Distributions of (a) turbulent kinetic energy and (b) rms pressure fluctuations from $x/R = 0.6$ to 1.0 . Here, red solid line denotes the trajectory of the tip-leakage vortex.

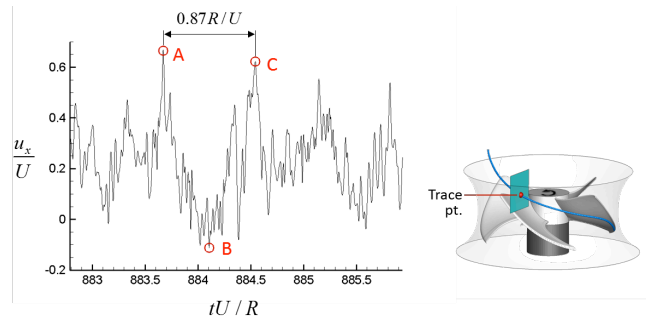


Figure 5. Time trace of the axial velocity at the core of the TLV near the pressure side of the blade (see a red circle on the schematic diagram).

B. UNSTEADY CHARACTERISTICS OF THE TLV

To analyze the time-dependent behavior of the TLV, figure 5 shows the time trace of the axial velocity at the core of the TLV near the pressure side of the blade. The velocity signal clearly shows low-frequency characteristics with high amplitudes and the corresponding Strouhal number, $St (= fU/R)$, is about 1. In Fig. 6, a time sequence of instantaneous flow fields on a meridional plane for a period from A to C in Fig. 5 is illustrated using velocity vector fields colored with the axial velocity and line contours of negative static pressure coefficient that shows an

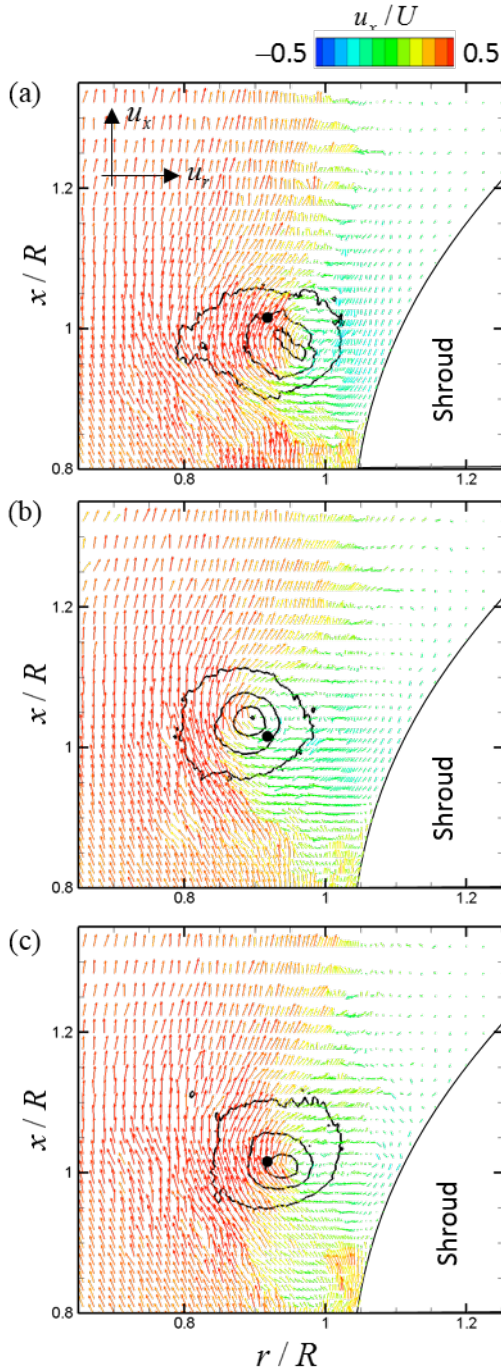


Figure 6. Evolution of the flow structures in time: (a), (b) and (c) correspond to A, B and C in Fig. 5, respectively. Here, line contours denote negative static pressure coefficients and a black dot denotes the mean core location.

instantaneous tip-leakage vortex. Flow around the tip-leakage vortex rotates in the clockwise direction. In Figs. 6(a) and (c), the core of instantaneous TLV locates on the right of the mean core location, and thus the flow at the mean core is accelerated because of clockwise rotation of the TLV, reaching maximum axial velocity at these time instants (A and C in Fig. 5). On the

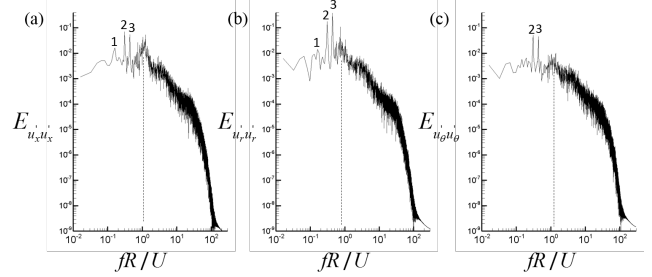


Figure 7. Frequency spectra of (a) axial, (b) radial and (c) azimuthal velocity fluctuations at the core of the TLV (see a red circle in Fig. 5). In (a)-(c), 1, 2 and 3 denote first three harmonics of fan revolution frequency.

other hand, in Fig. 6(b), the instantaneous TLV exists on the left of the mean core location, and decelerates the flow at the core location, reaching minimum axial velocity at the mean core location. These radial movements of the TLV generate low-frequency axial velocity fluctuations.

To examine the frequency characteristics of this oscillatory motion of the TLV, the energy spectra of three velocity components at the core of the TLV near the pressure side of the blade are computed (Fig. 7). Although the energy spectra show broadband characteristics, low-frequency peaks excluding harmonic frequencies of the fan revolution are observed for all velocity components. The non-dimensional frequency of this peak is $fR/U \sim 1$, corresponding to the period of oscillatory motion of the TLV. The peak frequency, $fR/U \sim 1$, is in good agreement with those of previous studies in the cascade (You et al., 2007) and other fans (Boudet et al., 2015; Pogorelov et al., 2015). By comparing the levels of the energy spectra, the axial and radial velocity fluctuations are dominant.

CONCLUSIONS

We performed LES of the flow in a rotating axial fan at the design condition of $Re = 547,000$ with an immersed boundary method in a non-inertial reference frame. The fan performance parameter from LES agreed well with those of experiments. Vortical structures such as the TLV, blade wake and edge separation were found. Among them, the TLV was the predominant flow structure. From the analysis of instantaneous flow fields and energy spectra of the velocity components at the core of the TLV, it was found that the TLV shows low-frequency wandering movement near the pressure side of the following blade.

ACKNOWLEDGEMENT

This research was supported by the KETEP (No. 20152020105600) of the MOTIE of Korea and also supported by the KISTI Supercomputing Center with supercomputing resources including technical support (KSC-2016-C3-0027).

REFERENCES

Akselvoll, K., and Moin, P., 1996, “An Efficient Method for Temporal Integration of the Navier–Stokes Equations in Confined Axisymmetric Geometries”, *Journal of Computational Physics*, Vol. 125, pp. 454–463.

Boudet, J., Cahuzac, A., Kausche, P., and Jacob, M. C., 2015, “Zonal Large-Eddy Simulation of a Fan Tip-Clearance Flow, With Evidence of Vortex Wandering”, *ASME Journal of Turbomachinery*, Vol. 137, p. 061001.

Hah, C., Hathaway, M., Katz, J., and Tan, D., 2015, “Investigation of Unsteady Tip Clearance Flow in a Low-Speed One and Half Stage Axial Compressor with LES and PIV”, *Proceedings, ASME-JSME-KSME Joint Fluids Engineering Conference*, pp. 166-178.

Jang, C., Furukawa, M., and Inoue, M., 2001, “Analysis of Vortical Flow Field in a Propeller Fan by LDV Measurements and LES – Part I: Three-Dimensional Vortical Flow Structures”, *ASME Journal of Fluids Engineering*, Vol. 123, pp. 748–754.

Jeong, J., and Hussain, F., 1995, “On the identification of a vortex”, *Journal of Fluid Mechanics*, Vol. 285, pp. 69-94.

Jin, G., Ouyang, H., and Du, Z., 2013, “Experimental Investigation of Unsteady Flow in Axial Skewed Fans According to Flow Rates”, *Experimental Thermal and Fluid Science*, Vol. 48, pp. 81-96.

Kim, D., and Choi, H., 2006, “Immersed Boundary Method for Flow around an Arbitrarily Moving Body”, *Journal of Computational Physics*, Vol. 212, pp. 662-680.

Lee, J., Choi, H., and Park, N., 2010, “Dynamic Global Model for Large Eddy Simulation of Transient Flow”, *Physics of Fluids*, Vol. 22, p. 075106.

Miorini, R. L., Wu, H., and Katz, J., 2012, “The Internal Structure of the Tip Leakage Vortex within the Rotor of an Axial Waterjet Pump”, *ASME Journal of Turbomachinery*, Vol. 134, p. 031018.

Park, N., Lee, S., Lee, J., and Choi, H., 2006, “A Dynamic Subgrid-Scale Eddy Viscosity Model with a Global Model Coefficient”, *Physics of Fluids*, Vol. 18, p. 125109.

Pogorelov, A., Meinke, M., and Schröder, W., 2015, “Cut-Cell Method Based Large-Eddy Simulation of Tip-Leakage Flow”, *Physics of Fluids*, Vol. 27, p. 075106.

Posa, A., Lippolis, A., Verzicco, R., and Balaras, E., 2011, “Large-Eddy Simulations in Mixed-Flow Pumps Using an Immersed-Boundary Method”, *Computers & Fluids*, Vol. 47, pp. 33-43.

Tan, D., Li, Y., Wilkes, I., Miorini, R. L., and Katz, J., 2015, “Visualization and Time-Resolved Particle Image Velocimetry Measurements of the Flow in the Tip Region of a Subsonic Compressor Rotor”, *ASME Journal of Turbomachinery*, Vol. 137, p. 041007.

You, D., Wang, M., Moin, P., and Mittal, R., 2007, “Vortex Dynamics and Low-Pressure Fluctuations in the Tip-clearance flow”, *ASME Journal of Fluids Engineering*, Vol. 129, pp. 1002-1014.